Phosphatidylinositol 4-phosphate 5-kinases 1 and 2 are involved in the regulation of vacuole morphology during *Arabidopsis thaliana* pollen development.

José-Manuel Ugalde[1], Cecilia Rodriguez-Furlán[2], Riet De Rycke[3], Lorena Norambuena[2], Jiří Friml[3,4], Gabriel León[1], Ricardo Tejos[2,4,5*]

[1]Laboratorio de Reproducción y Desarrollo de Plantas, Centro de Biotecnología Vegetal, Universidad Andrés Bello, 8370146 Santiago, Chile.

[2]Centro de Biologia Molecular Vegetal, Departamento de Biologia, Facultad de Ciencias, Universidad de Chile, 7800003 Santiago, Chile.

[3]Institute of Science and Technology Austria (IST Austria), 3400 Klosterneuburg, Austria.

[4]Department of Plant Systems Biology, VIB, and Department of Plant Biotechnology and Bioinformatics, Ghent University, 9052 Gent, Belgium.

[5]Departamento de Biologia, Facultad de Quimica y Biologia, Universidad de Santiago de Chile, Santiago, Chile.

*to whom correspondence should be addressed: Ricardo Tejos (ricardo.tejos@cbmv.cl or ricardo.tejos@usach.cl)

ABSTRACT

The pollen grains arise after meiosis of pollen mother cells within the anthers. A series of complex structural changes follows, generating mature pollen grains capable of performing the double fertilization of the female megasporophyte. Several signaling molecules, including hormones and lipids, have been involved in the regulation and appropriate control of pollen development. Phosphatidylinositol 4-phophate 5-kinases (PIP5K), which catalyze the biosynthesis of the phosphoinositide PtdIns(4,5)P_2, are important for tip polar growth of root hairs and pollen tubes, embryo development, vegetative plant growth, and responses to the environment. Here, we report a role of PIP5Ks during microgametogenesis. *PIP5K1* and *PIP5K2* are expressed during early stages of pollen development and their transcriptional activity respond to auxin in pollen grains. Early male gametophytic lethality to certain grade was observed in both *pip5k1*$^{-/-}$ and *pip5k2*$^{-/-}$ single mutants. The number of *pip5k* mutant alleles is directly related to the frequency of aborted pollen grains suggesting the two genes are involved in the same function. Indeed *PIP5K1* and *PIP5K2* are functionally redundant since homozygous double mutants did not render viable pollen grains. The loss of function of *PIP5K1* and *PIP5K2*results in defects in vacuole morphology in pollen at the later stages and epidermal root cells. Our results show that *PIP5K1*, *PIP5K2* and phosphoinositide signaling are important cues for early developmental stages and vacuole formation during microgametogenesis.

Keywords: pollen development, microgametogenesis, phosphoinositides, PIP5K, vacuole

1. INTRODUCTION

In flowering plants, male gametes develop inside male gametophytes structure, the pollen grains. The male gametophytes emerge after meiosis of diploid pollen mother cells within the anthers, generating a tetrad of haploid cells. The tetrad cells are then released as free microspores and undergo a series of complex processes that finally produce the mature pollen grain (MPGs). In *Arabidopsis thaliana*, an MPG consists of two generative cells encapsulated in the cytoplasm of a larger vegetative cell. While the last one contributes to the MPG survival and pollen tube formation, the two smaller germline cells participate in the ovule fertilization that will produce the zygote, the endosperm and seed tissues [1].

Microspore development is tightly associated with processes of cell wall deposition and vacuole biogenesis. After the first pollen mitosis, pre-existing small vacuoles fuse into a large vacuole before the generative cell formation. Later on, after the second mitosis, the mature tricellular pollen contains small dispersed vacuoles [1]. This progression in vacuole biogenesis must be tightly regulated during pollen development to appropriately control pollen growth and maturation.

In yeast, vacuole biogenesis dynamics requires a set of lipids that play regulatory roles in vesicle trafficking and membrane fusion, including phosphatidylinositol 3-phosphate (PtdIns3P), phosphatidylinositol 4,5-bisphosphate (PtdIns(4,5)P_2), diacylglycerol (DAG) and phosphatidic acid (PA) [2-6]. The abundance and metabolism of these lipids play important roles in lipid signaling and membrane trafficking. Phosphatidylinositol metabolism determines the relative abundance of each lipid in intracellular compartments and defines the identity of vesicles and directionality of membrane trafficking. In Arabidopsis, the impairment of genes implicated in phosphatidylinositol metabolism has deleterious consequences on the function and morphology of vacuoles. The overexpression of the phosphatases *Suppressor of Actin (SAC)* genes, which are presumably involved in the metabolism of PtdIns(3,5)P_2 to PtdIns3P, leads to larger and fewer vacuoles in root tips, whereas decreased *SAC* expression has the opposite effect [2]. In *sac* loss and gain of function mutants, endocytic and vacuolar trafficking of the auxin efflux carrier PINFORMED2 (PIN2) is impaired, suggesting that the protein trafficking to the vacuole also depend on the levels of PtdIns(3,5)P_2 and PtdIns3P [2]. Two out of the four Arabidopsis PtdIns3P 5-kinase genes, *FAB1A* and *FAB1B* are expressed in pollen. The double mutant *fab1a*$^{-/-}$ *fab1b*$^{-/-}$ exhibits pollen lethality as a consequence of a failure in vacuole rearrangement [3]. Thus,

PtdIns3P and PtdIns(3,5)P_2 synthesis is crucial for vacuole morphogenesis and essential for proper male gametophyte development. Nevertheless, little information exists on the role of other phosphoinositides in plant vacuole dynamics and during microgametogenesis.

Here, we present evidence indicating that the enzymes PIP5K1 and PIP5K2, which are involved in the synthesis of PtdIns(4,5)P_2, are essential for early pollen development. The single homozygous *pip5k1*$^{-/-}$ and *pip5k2*$^{-/-}$ as the double heterozygous mutant *pip5k1*$^{+/-}$*pip5k2*$^{+/-}$ display defects during early microgametogenesis generating pollen grain abortion. Pollen grains from flowers of the *pip5k1*$^{+/-}$*pip5k2*$^{+/-}$mutants show defects in vacuoles and exine wall formation. These vacuole defects of pollen are consistent with the defects observed in vacuole morphology and protein trafficking in root cells of *pip5k1*$^{-/-}$*pip5k2*$^{-/-}$ mutants. Overall our data suggest that PIP5K1 and PIP5K2 are important for vacuole biogenesis and early pollen development.

2. RESULTS

2.1. ***PIP5K1*** **and** ***PIP5K2*** **are expressed during early pollen development and their transcript levels increased in response to auxin.**

In *Arabidopsis thaliana*, phosphatidylinositol 4-phosphate 5-kinases (PIP5K) form of a family of 11 members (PIP5K1 – PIP5K11) [4] which are functionally redundant [5–7]. *PIP5K1* and *PIP5K2* are part of the subgroup of ubiquitously expressed *PIP5Ks*. Both genes are expressed in several developmental contexts, including seedlings, embryos, root tips, leaves, and inflorescence stems [5,7]. Interestingly, *PIP5K1* and *PIP5K2* transcripts were also detected in closed and open flowers (Supplementary Figure 1A), suggesting they may be expressed during early and late stages of gametogenesis. We checked published transcriptomic data from different microgametogenesis developmental stages and found *PIP5K1* and *PIP5K2* are expressed early in pollen development in unicellular microspores (UNMs) and bicellular pollen (BCP) (Supplementary Table 1, [8]). We confirmed the pollen expression for *PIP5K1* and *PIP5K2* using promoter transcriptional reporters lines [7]. These lines confirmed the activity of the *PIP5K1* and *PIP5K2* promoters at the tetrad, bicellular (BCP) and tricellular (TCP) pollen developmental stages (Figure 1), indicating they may perform an important function during reproductive development.

During pollen development, auxin plays a fundamental regulatory role. Auxin maxima are detected from the UNM to TCP stages, which declines when pollen maturation and anther dehiscence begins [9–12]. Despite the relatively important role of auxin and the myriad of different signalling pathways regulated by auxin during different aspects of plant development, no gene candidates downstream of auxin signaling have been characterized in the context of microgametogenesis so far. Both *PIP5K1* and *PIP5K2* were previously reported as auxin-inducible genes in other developmental contexts [7,13], hence, we tested whether auxin is able to induce *PIP5K1* and *PIP5K2* transcript accumulation in pollen as well. Interestingly, *PIP5K1* and *PIP5K2* expression was also induced by exogenous application of indole 3-acetic acid (IAA) in pollen grains from open flowers (Supplementary Figure 1B). Pretreatment with cycloheximide (CHX) abolished the ability of IAA to stimulate pollen *PIP5K1* and *PIP5K2* transcript accumulation suggesting that they are downstream targets of the primary auxin-controlled genes. So far these are first examples of auxin inducible genes in pollen grains.

2.2. Microgametogenesis is altered in *pip5k1* and *pip5k2* mutants.

The loss of function of both *PIP5K1* and *PIP5K2* leads developmental defects. The double homozygous *pip5k1*$^{-/-}$*pip5k2*$^{-/-}$ mutants displays shorter primary roots, reduced apical root meristems size, reduced lateral root number, and increased levels of anthocyanins in cotyledons and leaves compared to wild type [5,7]. Additionally, the *pip5k1*$^{-/-}$*pip5k2*$^{-/-}$ seedlings generate unfertile adult plants [5,7] suggesting essential roles of *PIP5K1* and *PIP5K2* during reproductive development. Due to the observation of *PIP5K1* and *PIP5K2* expression in microgametogenesis (Figure 1), we decided to further analyze the gametogenesis in *pip5k* mutants. Since the *pip5k1*$^{-/-}$*pip5k2*$^{-/-}$ is unfertile the phenotypes were characterized in the double heterozygote *pip5k1*$^{+/-}$*pip5k2*$^{+/-}$ as well in the homozygous/heterozygous combinations *pip5k1*$^{+/-}$*pip5k2*$^{-/-}$ and *pip5k1*$^{-/-}$*pip5k2*$^{+/-}$, which were all producing viable fertile plants and fairly normal vegetative and flower growth. Also single heterozygous and homozygous mutants of *PIP5K1* and *PIP5K2* were included in the analysis. We observed that the size of the siliques, directly related to the number of seeds produced, was affected when either *PIP5K1* or *PIP5K2* was mutated. Interestingly, the severity the silique defect of *pip5k* mutants depended on the number of functional alleles of *PIP5K1* and *PIP5K2* present in the plant (Figure 2). The *pip5k1*$^{+/-}$*pip5k2*$^{-/-}$ and *pip5k1*$^{-/-}$*pip5k2*$^{+/-}$ mutants displayed the smallest silique size and produced only a few seeds per silique, indicating a defect during gametogenesis.

Between *pip5k1*$^{+/-}$*pip5k2*$^{-/-}$ and *pip5k1*$^{-/-}$*pip5k2*$^{+/-}$ mutant lines, the lack of function of *PIP5K2* seems to have a stronger effect on the number of seeds than *PIP5K1* loss-of-function. Out of the eleven Arabidopsis *PIP5Ks*, besides *PIP5K1* and *PIP5K2*, also *PIP5K4*, *PIP5K5*, *PIP5K6* and *PIP5K8* transcripts had been detected during pollen development (Supplementary Table 1, [8]). However, the impairment of *PIP5K1* and *PIP5K2* rendered a strong impact on pollen and seed formation suggesting that the other *PIP5K* may have different functions in this developmental context. Consistently with this idea, the *PIP5K1* and *PIP5K2* loss-of-function mutants exhibit empty spots in their siliques which increased in frequency as the number of mutant alleles increases, showing a positive correlation with the reduction in the silique size and seed set (Figure 2). These phenotypes were indicative of either a failure of the fertilization or a specific defect in gametophyte development. However, examination of dissected pistils of the different mutant revealed no detectable defects in ovule number or development (data not shown). Therefore most likely the loss of function of *PIP5K1* and *PIP5K2* provoked specific defects in male gametophytes.

The defect on seed setting prompted us to analyze pollen development in detail (Figure 3). Pollen viability was assayed in fresh pollen isolated from all the *pip5k1* and *pip5k2* mutants coombinations. The *pip5k1*$^{+/-}$*pip5k2*$^{-/-}$ double mutant displayed a high frequency of completely collapsed pollen grains (Figures 3B and 3D). To determine the contribution of each mutant allele for the defects in pollen grain formation, we estimated the proportion of aborted pollen grains in the combination of one, two or three *PIP5K1* and *PIP5K2* mutant alleles (Figure 3E). The single heterozygous *pip5k1*$^{+/-}$ *or pip5k2*$^{+/-}$ mutants showed around 10% of aborted unviable pollen grains. The percentage of unviable pollen increased to around 30% in the single homozygous mutants *pip5k1*$^{-/-}$ *or pip5k2*$^{-/-}$ (Figure 3E) indicating that the absence in either *PIP5K1* or *PIP5K2* do not produce a fully-penetrant gametophytic lethal phenotype. When we analyzed two mutant alleles in the heterozygous *pip5k1*$^{+/-}$*pip5k2*$^{+/-}$ double mutant we observed 35.1% of unviable pollen. Increasing the number of mutant alleles in *pip5k1*$^{+/-}$*pip5k2*$^{-/-}$ or *pip5k*$^{-/-}$*pip5k2*$^{+/-}$ mutants the defect reached 36.5% and 50.2% of unviable pollen, respectively. The evidence showed a positive correlation between the number of *PIP5K1* or *PIP5K2* mutant alleles and the defect of pollen grains viability consistently with the phenotypes observed in seed set (Figure 2). However, the percentages of pollen abortion were lower to what is expected for a

single mutant allele displaying a fully-penetrant gametophytic lethal phenotype (see Supplementary table 2 for data comparisons). Considering that other *PIP5K* genes homologues are also expressed in pollen (Supplementary Table 1), the difference in penetrance could be attributed to a partial redundancy among the *PIP5K* family due to differences in expression levels or spatio-temporal expression and/or enzymatic properties and efficiency (e.g. *PIP5K1* could replace more efficiently the function of *PIP5K2*, and not the opposite).

To further characterize the phenotypes in pollen development, we carried out cytological observations on toluidine blue-stained anther sections from chemically fixed floral tissues of double heterozygous *pip5k1*$^{+/-}$*pip5k2*$^{+/-}$mutant plants (Figure 4). We used double heterozygous mutants as they show a good pollen phenotype penetrance and to avoid any pollen defect arising from the mutant sporophyte. The first clearly visible difference between wild type and the anthers from the mutant plants was detectable early during the tetrad stage. We distinguished abortion of microspores, spotted as dark-stained structures in anthers at stage 5 (Figure 4C; Anther developmental stages defined as Sanders et al. [14]). These defects were also observed later in anther development, including the stage 13 were mature pollen grains are released from the pollen sacs (Figures 4D). In wild type anthers, homogeneous pollen population were observed; with round pollen grains showing a dense cytoplasm (Figure 4B). In contrast, anthers from mutant plants contained heterogeneous pollen grains, ranging from normal wild type phenotype to pollen grains where the cytoplasm was detached from the cell wall or pollen grains were wrinkled and totally collapsed (Figure 4D). Due to the genotype used in this analysis, we are unable to clearly state the genotype of each pollen grain observed. Nevertheless, this assay is a good approach to obtain information on the developmental stage where pollen grains began to show abnormalities.

Altogether, these data indicates that *PIP5K1* and *PIP5K2* have an important function during early stages of microgametogenesis, showing an essential role for these phosphoinositide kinases for proper pollen development. Additionally, the function of *PIP5K1* and *PIP5K2* seems to be redundant to others members of the *PIPK* family.

2.3. The loss of function of *PIP5K1* and *PIP5K2* produces defects on vacuoles and exine wall in pollen grains.

The vacuole growth is thought to be the driving force for the early vegetative expansion of the unicellular microspore. The unique very large vacuole present in early microgametogenesis gets

fragmented after the first mitotic division and the resulting small vesicles further change their structural and functional characteristics [15,16]. On the other hand, phosphoinositides influence the formation of vacuoles during pollen development [3,17]. According to this, we were interested in studying vacuolar morphology in pollen in the *PIP5K1* and *PIP5K2* loss-of-function plants. Again, we chose to use the *pip5k1*$^{+/-}$*pip5k2*$^{+/-}$ double heterozygous mutant was analyzed to reduce the possible effect of mutant sporophytic tissues on the phenotype. Pollen vacuoles were visualized using neutral red staining which rapidly accumulates inside vacuoles and other acidic compartments. Mature wild type pollen grains stained with neutral red exhibited numerous small vacuolar structures (Figure 5A). In contrast, pollen grains obtained from *pip5k1*$^{+/-}$*pip5k2*$^{+/-}$ mutant plants displayed fewer and abnormally large vacuoles (Figure 5B). This abnormal phenotype was observed in 10.4% of the analyzed pollen sample. Unfortunately, it is undoable to differentiate the genotype of the defective and normal pollen grains observed. However, the ratio of defective pollen points out to a defect most probably arisen from the pollen grain itself and not from the wild type-like double heterozygous anther tissues.

Additional pollen morphology phenotypes were observed using transmitted electron micrographs in cryo-fixed anthers collected from open flowers obtained from *pip5k1*$^{+/-}$*pip5k2*$^{+/-}$ mutant plants. Pollen grains isolated from mutant plants often displayed smaller and less complex exine walls compared to pollen grains obtained from wild type flowers (Figures 5D, and 5G). Additionally, pollen grains isolated from *pip5k1*$^{+/-}$*pip5k2*$^{+/-}$ flowers displayed increased abundance of intracellular organelles, such as mitochondria and plastids, and also more and larger vacuoles (Figures 5D and 5H). The data suggested that the loss of function of *PIP5K1* and *PIP5K2* resulted in defects during vacuolar morphogenesis as well as biogenesis of mitochondria, plastids, and other organelles. The defective exine wall formation could be due to further abnormalities during secretion of the pollen outer cell wall as previously described in other developmental contexts [18].

2.4. *PIP5K1* and *PIP5K2* are involved in protein trafficking to the vacuole in root tip epidermal cells.

The double homozygous mutant *pip5k1*$^{-/-}$*pip5k2*$^{-/-}$ generates unfertile adult plants making impossible to analyze the vacuole phenotypes in pollen grains and to be sure about their genotype. However, as few double *pip5k1*$^{-/-}$*pip5k2*$^{-/-}$ do escape lethality, we analyzed the morphological defects in vacuoles in epidermal cells in the root tips. In these cells, the dye

lysotracker red had been useful to visualize acidic compartments such as vacuoles, lysosomes, and prevacuolar compartments using confocal microscopy. Double homozygous *pip5k1*$^{-/-}$*pip5k2*$^{-/-}$ mutants were preselected based on their size and morphology at seven day-after germination [7]. The lysotracker red staining in *pip5k1*$^{-/-}$*pip5k2*$^{-/-}$ seedlings showed smaller vacuoles in root epidermal cells as compared to wild type stained controls (Figure 6A). As vacuolar morphology and biogenesis are tightly regulated by trafficking events, we analyzed the protein trafficking toward the vacuole using the fungal toxin Brefeldin A (BFA) and the well-characterized protein marker for intracellular trafficking, the auxin carrier PINFORMED1(PIN1)[19]. BFA restrains PIN1 recycling from endosomal compartments to the plasma membrane and leads to its accumulation in aggregated endosomes, typically called BFA bodies [20]. Depending on the BFA concentration, the vacuolar trafficking could also be inhibited [21], allowing the differential interference with these two trafficking pathways. When BFA was used at a concentration which inhibits exocytosis and vacuolar trafficking (i.e. 50 μM for 90 min), we observed larger PIN1 BFA-bodies in the *pip5k1*$^{-/-}$*pip5k2*$^{-/-}$ mutants compared to wild type seedlings (Figure 6B and 6C). Treatments with 25 μM BFA targets preferentially PIN1 recycling to the plasma membrane and does not abolish trafficking to the vacuole [21]. This treatment in *pip5k1*$^{-/-}$*pip5k2*$^{-/-}$ resulted in smaller PIN1 BFA-bodies suggesting that PIN1 trafficking from the plasma membrane to the vacuole is enhanced in the loss of function of *PIP5K1* and *PIP5K2* (Figure 6B and 6C). Therefore, *PIP5K1* and *PIP5K2* are involved in vacuole morphogenesis and play a role regulating protein trafficking to the vacuole in root epidermal cells, pointing to a broader role of these phosphoinositide kinases in vacuolar function during plant development.

3. DISCUSSION

Phosphoinositides are lipid molecules involved in almost every aspect of membrane processes in higher organisms. PtdIns(4,5)P_2 is produced by PIP5K-mediated phosphorylation at the position 5 of the inositol ring in PtdIns4P. We have previously found that PIP5K1 and PIP5K2 are redundantly required for auxin distribution, PIN polarity, and tissue patterning [7]. Here we further report that PIP5K1 and PIP5K2 are redundantly acting during early stages of microgametogenesis presumably downstream of the auxin signaling necessary for pollen grain

formation. We also demonstrate that these two enzymes are involved in vacuolar morphogenesis and in the regulation of protein trafficking toward the vacuole.

3.1. PIP5K1 and PIP5K2 are involved in pollen development

Phosphoinositides isomers and their differential subcellular localization are important factors for multiple cellular processes in all eukaryotes. In plant cells, the phosphoinositide PtdIns(4,5)P_2 is a phospholipid present in a very low amount, yet the Arabidopsis genome contains eleven PIP5K enzymes that form a highly redundant class of proteins. For instance, PIP5K4/5 and PIP5K10/11 have redundant functions during pollen tube elongation [18,22]. PIP5K1/2 also form a pair of functionally redundant proteins during auxin-dependent embryo development [7]. Here we have characterized their redundant role during pollen development. The increased percentage of aborted pollen grains was found to be in direct relationship to the number of *pip5k1* and *pip5k2* mutant alleles in the different genotype combinations analyzed. These alterations caused defects in seed set, generating shorter siliques containing fewer seeds. Moreover, the fact that it is possible to obtain double homozygous *pip5k1*$^{-/-}$ *pip5k2*$^{-/-}$ mutant seedlings, although they are unable to produce flowers, highlights the partial penetrance of the phenotypes and the further redundancy in function with other pollen-expressed *PIP5Ks* (Supplementary table 2). Additionally, the cytological analysis indicates that microspores collapse as early as the tetrad stage suggesting that PIP5K1 and PIP5K2 play an important role during early microgametogenesis.

The phytohormone auxin participates in pollen development and components of auxin biosynthesis, signaling, and transport are also present throughout microgametogenesis [23–25]. Additionally, it has been reported that auxin increases the PtdIns(4,5)P_2 content at the plasma membrane in Arabidopsis roots [7]. The auxin effect on PtdIns(4,5)P_2 accumulation in roots can be partially explained by an increase in *PIP5Ks* transcription because the response is reduced in the double knockout mutant *pip5k1*$^{-/-}$ *pip5k2*$^{-/-}$ background [7]. Auxin is also able to induce the transcript accumulation of *PIP5K1* and *PIP5K2* in pollen and this effect seems to be indirect and needs the synthesis of additional protein factors. Thus, as it occurs in roots, auxin in pollen acts regulating *PIP5K1* and *PIP5K2* transcript accumulation, and presumably also inducing an increase in PtdIns(4,5)P_2. Nevertheless, to date, there is not a single example of downstream components of auxin response that could give a glimpse about auxin function during microgametogenesis. It would be of interest to further analyze whether any component of auxin

synthesis or signaling has defects in early pollen development. Alternatively, finding the unknown transcription factor involved in the auxin transcriptional response of *PIP5K* would shade light on a so far poorly characterized mechanism of pollen grain development depending on auxin and phosphoinositides.

3.2. PIP5K1 and PIP5K2 are involved in vacuolar morphogenesis and in the regulation of protein trafficking to the vacuole.

Several players and molecular mechanisms that contribute to plant vacuole biogenesis, including vesicle trafficking and fusion of vacuolar membranes, have been related to the phosphatidylinositol metabolism. Mutants in *AtVPS34* and *AtVPS15*, both necessary to catalyze the biosynthesis of PtdIns3P, also exhibit severe pollen developmental defects and changes in vacuole morphology [17,26,27]. Furthermore, the *fab1a* $^{-/-}$ *fab1b* $^{-/-}$ double knockout mutants, which are deficient in PtdIns3P 5-kinase activity, presented similar pollen and vacuolar phenotypes [9,28]. Additionally, reduced expression levels of *FAB1A* and *FAB1B* caused vacuole morphological abnormalities and impaired vacuolar acidification in pollen grains, and additionally seedlings displayed several root phenotypes including an incorrect localization of auxin transporters, growth inhibition, hyposensitivity to exogenous auxin, and disturbance of root gravitropism [29,30]. These data support the crucial role for PtdIns3P and PtdIns(3,5)P_2 in modulating the dynamics of vacuolar rearrangement in plant cells and implies that disruption of vacuolar dynamics impacts pollen development. The evidence presented here involved the synthesis of the phosphoinositide PtdIns(4,5)P_2 in vacuolar morphogenesis as an essential process for pollen development. In concordance, previous studies in yeast indicated that both PtdIns3P and PtdIns(4,5)P_2 regulate vacuole function [31–33]. As the vacuolar phenotype in pollen and root epidermal cells observed in *pip5k1* and *pip5k2* mutants present similarities with those involved in the biosynthesis of PtdIns(3,5)P_2, there is the possibility that PIP5Ks also utilizes PtdIns3P as a substrate. However, based on plant PIP5K protein structural characteristics the only plausible alternative is the phosphorylation of PtdIns4P and not of PtdIns3P [4]. Moreover, *in vitro* assays showed that PIP5K1 is able to synthesize only PtdIns(4,5)P_2 and PtdIns(3,4,5)P_3, the later most likely not present in *Arabidopsis* [34]. Therefore, most probably the vacuolar phenotype arise as a direct consequence of the lack of PtdIns(4,5)P_2 or the over-accumulation of PtdIns4P, placing PtdIns(4,5)P_2 as a new phospholipid involved in vacuolar function in plants.

Vacuole fusion events are tightly related to trafficking events that involve tethering, docking and membrane fusion processes [10,35]. Several pieces of evidence support the hypothesis that trafficking to the vacuole is regulated by phosphoinositides and their depletion is the main cause for vacuole morphological alterations [2,36,37,40]. Specifically, auxin cause an increase in PtdIns(4,5)P_2 and a concomitant decrease of PtdIns4P, the PIP5Ks most probable substrate . This auxin effect on PtdIns4P/PtdIns(4,5)P_2 ratio is dependent on the activity of PIP5K1and PIP5K2 as the phosphoinositide response is reduced in the *pip5k1*$^{-/-}$*pip5k2*$^{-/-}$ double homozygous mutant background [7]. These changes on PtdIns4P and PtdIns(4,5)P_2 levels at the plasma membrane have been linked to the regulation of the vacuolar morphology in roots [7, 40]. Here we have also showed that protein trafficking to the vacuole is also affected in the *pip5k1*$^{-/-}$*pip5k2*$^{-/-}$ mutant seedlings evidenced by an accumulation of PIN1-containing BFA bodies in root cells. Furthermore, the vacuoles in *pip5k1*$^{-/-}$*pip5k2*$^{-/-}$ mutant root tips are considerable smaller in size and number. Recent studies have pointed out to a transcriptional regulatory role of auxin on vacuole morphology and PIN trafficking toward the vacuole in epidermal root cells [38, 40]. Nevertheless, there is no evidence showing that auxin can also modulate vacuolar morphology in pollen, but our data showing *PIP5K1* and *PIP5K2* are transcriptionally controlled by auxin place the phosphoinositide-dependent pathway as a plausible mechanism by which auxin modulates vacuolar function in pollen and microgametogenesis. Taken together, all our data suggest that PIP5Ks and PtdIns(4,5)P_2, may be regulating trafficking and morphogenesis of the vacuole. Further studies are required to identify potential binding partners for PtdIns(4,5)P_2 and to explore the metabolism of this phosphoinositide or its derivatives in the vacuolar function in detail.

4. MATERIAL AND METHODS

4.1. Plant material and growth conditions

All *Arabidopsis thaliana* lines are in the Col-0 background. The mutant lines *pip5k1*$^{-/-}$ (SALK_146728) and *pip5k2*$^{-/-}$ (SALK_012487), all the double mutant combinations, together with the transcriptional reporter lines pPIP5K1:nlsGUS-GFP and pPIP5K2:nlsGUS-GFP, were previously published [5,7]. The *pip5k1*$^{-/-}$ and *pip5k2*$^{-/-}$ mutants were crossed to each other and the different genotypes were obtained and selected from F2 and F3 populations by PCR using the primers listed in Supplementary Table 3.

Seeds were sterilized overnight by chlorine gas or with a 50% solution of commercial bleach and then rinsed with abundant sterile water. Sterilized seeds were sown on solid Arabidopsis medium (0.5X Murashige and Skoog basal salts, 1% sucrose and 0.8% agar, pH 5.7) and stratified at 4°C for at least two days prior to transfer to a light/dark cycle of 16/8h 18°C growth regime. For root assays, seedlings were grown vertically for 4 to 12 days prior to analysis. For pollen analyses, one-week-old seedlings germinated on solid media were transferred to hydroponic medium and grown until flowering (6-10 weeks) in a growth chamber with controlled temperature at 22°C and a light/dark cycle of 16h/8h.

All primer used for expression analyses and *pip5k* mutant genotyping are listed in Supplementary Table 3.

4.2. Pollen analysis

For the histological analysis, flowers were collected and fixed overnight in 3% glutaraldehyde solution in 0.1 M sodium cacodylate (pH 7.2), then dehydrated in acetone series and embedded in Epon resin (Embed 812, Electron Microscopy Sciences, USA) following manufacturer's instructions. Anther 2 µm transverse sections were stained with 1% toluidine blue. Alexander staining [Malachite green 0,05% (w/v), acid fuchsine 0,05% (w/v), orange G 0.005% de (w/v), phenol 5% (w/v), acetic acid 2% (v/v), glycerol 25% (v/v), and ethanol 50% (v/v)] and neutral red staining [neutral red 0,01 % (w/v) in 8% sucrose (w/v)] were performed on glass slides, incubating dissected anthers for 5 min in the respective staining solution.. Stained pollen and anther cross sections were visualized by using the Olympus IX81 microscope and bright-field photographs were taken using a MicroPublisher 3.3 RTV digital camera.

Confocal images of pollen at different stages were obtained after collecting pollen grains by gently pressing flowers over a microscope slide containing an 8% sucrose (w/v) solution. Pollen grains were immediately imaged using a Zeiss 710 laser scanning confocal microscope.

4.3. Pollen transmission electron microscopy analysis

Anthers were collected from wild type and *pip5k1*$^{+/-}$*pip5k2*$^{+/-}$ plants into a 20% (w/v) bovine serum albumin (BSA) solution using 1 mm needles under a binocular microscope. Anthers were frozen immediately in a high-pressure freezer (EM PACT; Leica Microsystems). Freeze substitution was carried out in a Leica AFS (Leica Microsystems). Over a period of 4 days, samples were freeze-substituted in dry acetone as follows: –90°C for 26 h, 2°C increase per hour for 15 h, –60°C for 16 h, 2°C increase per hour for 15 h, and –30°C for 8 h. Afterwards, samples were slowly warmed up to 4°C, infiltrated stepwise over 3 days at 4°C in Spurr's resin, and embedded in capsules. Resin polymerization was performed at 70°C for 16 h. Ultrathin sections of gold interference color were cut with an ultramicrotome (EM UC6; Leica Microsystems) and collected on formvar-coated copper mesh grids. Sections were post-stained in a Leica EM AC20 for 30 min in uranyl acetate at 20°C and for 7 min in lead stain at 20°C. Grids were viewed with a JEM 1010 transmission electron microscope (JEOL) operating at 80 kV.

4.4. Immunohistochemistry and live root cell assays.

Whole mount immunolocalization studies were performed as previously described [39] using rabbit antiPIN1 antibody diluted 1 to 1000 and anti-Rabbit IgG coupled to Cy3 (Sigma) secondary antibodies diluted 1 to 600. For acidic compartments staining in root epidermal cells, seven day-old seedlings were incubated for one hour in liquid media containing 10 µM Lysotracker Red (Lifetechnologies). Seedlings were mounted in liquid growth media for imaging. All images were obtained with a Zeiss 710 laser scanning confocal microscope using a 63X water-immersion lens and standard filter sets.

4.5. Transcript levels analysis

RNA was isolated from different tissues using commercial TRIzol reagent (Invitrogen). To extract pollen RNA, pollen grains were collected from 50 to 100 complete inflorescences by softly grinding them in a mortar with 0.3 M Mannitol. The pollen extract was filtered using two

sequential Nylon meshes (Nitex) of 80 µm and 35 µm pore size. Then the filtered pollen suspension was centrifuged for 7 min at 450*g*. Isolated pollen grains were incubated for 12 hours in 100 µL of 0.3 M Mannitol supplemented with combinations of 100 µM IAA and 50µM CHX. After incubation, glass beads were used to grind the pollen grains and RNA extraction was performed using the RNeasy Plant mini RNA extraction kit (Qiagen). cDNA was synthesized using 1 µg of DNAase-treated RNA using the Super Script II First Strand Synthesis Kit (Invitrogen). Quantitative PCR was performed using primer listed in Supplementary Table 3 with the Fast Eva green qPCR master mix (Biotium) using 95 °C for 10 min and 40 cycles of 95 °C for 10 sec, 60 °C for 15 sec, and 72 °C for 20 sec. For normalizing the transcript levels, we used a pentatricopeptide protein coding gene (At5g55840). The results were analyzed using the software MxPro – Mx3000P v4.1 Build 389 (Schema 85).

5. ACKNOWLEDGEMENTS

We thank Dr. Glenn Hicks for his comments on the manuscript. This work was supported by the National Commission for Scientific and Technological Research, PAI grant number [PAI82130047] to RT, the National Fund for Scientific and Technological Research project numbers[11080037] to GL and [1120289] to LNM, and the Odysseus Program of the Research Foundation-Flanders [G091608] to JF.

6. REFERENCES

[1] Y. Hamamura, S. Nagahara, T. Higashiyama, Double fertilization on the move., Curr. Opin. Plant Biol. 15 (2012) 70–7. doi:10.1016/j.pbi.2011.11.001.

[2] P. Nováková, S. Hirsch, E. Feraru, R. Tejos, R. van Wijk, T. Viaene, et al., SAC phosphoinositide phosphatases at the tonoplast mediate vacuolar function in Arabidopsis., Proc. Natl. Acad. Sci. U. S. A. 111 (2014) 2818–23. doi:10.1073/pnas.1324264111.

[3] P. Whitley, S. Hinz, J. Doughty, Arabidopsis FAB1/PIKfyve proteins are essential for development of viable pollen., Plant Physiol. 151 (2009) 1812–22. doi:10.1104/pp.109.146159.

[4] B. Mueller-Roeber, C. Pical, Inositol Phospholipid Metabolism in Arabidopsis . Characterized and Putative Isoforms of Inositol Phospholipid Kinase and Phosphoinositide-Specific Phospholipase C 1, Plant Physiol. 130 (2002) 22–46. doi:10.1104/pp.004770.22.

[5] T. Ischebeck, S. Werner, P. Krishnamoorthy, J. Lerche, M. Meijón, I. Stenzel, et al., Phosphatidylinositol 4,5-bisphosphate influences PIN polarization by controlling clathrin-mediated membrane trafficking in Arabidopsis., Plant Cell. 25 (2013) 4894–4911.

doi:10.1105/tpc.113.116582.

[6] T. Ischebeck, S. Seiler, I. Heilmann, At the poles across kingdoms: phosphoinositides and polar tip growth., Protoplasma. 240 (2010) 13–31. doi:10.1007/s00709-009-0093-0.

[7] R. Tejos, M. Sauer, S. Vanneste, M. Palacios-Gomez, H. Li, M. Heilmann, et al., Bipolar Plasma Membrane Distribution of Phosphoinositides and Their Requirement for Auxin-Mediated Cell Polarity and Patterning in Arabidopsis., Plant Cell. 26 (2014) 2114–2128. doi:10.1105/tpc.114.126185.

[8] D. Honys, D. Twell, Transcriptome analysis of haploid male gametophyte development in Arabidopsis, Genome Biol. 5 (2004) R85. doi:10.1186/gb-2004-5-11-r85.

[9] R. Aloni, E. Aloni, M. Langhans, C.I. Ullrich, Role of auxin in regulating Arabidopsis flower development., Planta. 223 (2006) 315–28. doi:10.1007/s00425-005-0088-9.

[10] Y. Cheng, X. Dai, Y. Zhao, Auxin biosynthesis by the YUCCA flavin monooxygenases controls the formation of floral organs and vascular tissues in Arabidopsis, Genes Dev. 20 (2006) 1790–1799. doi:10.1101/gad.1415106.molecular.

[11] X.-L. Feng, W.-M. Ni, S. Elge, B. Mueller-Roeber, Z.-H. Xu, H.-W. Xue, Auxin flow in anther filaments is critical for pollen grain development through regulating pollen mitosis, Plant Mol. Biol. 61 (2006) 215–26. doi:10.1007/s11103-006-0005-z.

[12] V. Cecchetti, M.M. Altamura, G. Falasca, P. Costantino, M. Cardarelli, Auxin regulates Arabidopsis anther dehiscence, pollen maturation, and filament elongation, Plant Cell. 20 (2008) 1760–74. doi:10.1105/tpc.107.057570.

[13] Y. Mei, W.-J. Jia, Y.-J. Chu, H.-W. Xue, Arabidopsis phosphatidylinositol monophosphate 5-kinase 2 is involved in root gravitropism through regulation of polar auxin transport by affecting the cycling of PIN proteins, Cell Res. 22 (2012) 581–97. doi:10.1038/cr.2011.150.

[14] P.M. Sanders, A.Q. Bui, K. Weterings, K.N. McIntire, Y.-C. Hsu, P.Y. Lee, et al., Anther developmental defects in Arabidopsis thaliana male-sterile mutants, Sex. Plant Reprod. 11 (1999) 297–322. doi:10.1007/s004970050158.

[15] Y. Yamamoto, M. Nishimura, I. Hara-nishimura, T. Noguchi, Behavior of Vacuoles during Microspore and Pollen Development in Arabidopsis thaliana, Plant Cell Physiol. 44 (2003) 1192–1201. doi:10.1093/pcp/pcg147.

[16] E. Pacini, C. Jacquard, C. Clément, Pollen vacuoles and their significance, Planta. 234 (2011) 217–27. doi:10.1007/s00425-011-1462-4.

[17] Y. Lee, E.-S. Kim, Y. Choi, I. Hwang, C.J. Staiger, Y.-Y. Chung, et al., The Arabidopsis phosphatidylinositol 3-kinase is important for pollen development., Plant Physiol. 147 (2008) 1886–97. doi:10.1104/pp.108.121590.

[18] T. Ischebeck, I. Stenzel, I. Heilmann, Type B phosphatidylinositol-4-phosphate 5-kinases mediate Arabidopsis and Nicotiana tabacum pollen tube growth by regulating apical pectin secretion, Plant Cell. 20 (2008) 3312–3330. doi:10.1105/tpc.108.059568.

[19] J. Petrásek, J. Mravec, R. Bouchard, J.J. Blakeslee, M. Abas, D. Seifertová, et al., PIN proteins perform a rate-limiting function in cellular auxin efflux, Science. 312 (2006) 914–918. doi:10.1126/science.1123542.

[20] N. Geldner, J. Friml, Y.-D. Stierhof, G. Jurgens, K. Palme, Auxin transport inhibitors block PIN1 cycling and vesicle trafficking, Nature. 413 (2001) 425–428. doi:10.1038/35096571.

[21] J. Kleine-Vehn, J. Leitner, M. Zwiewka, M. Sauer, L. Abas, C. Luschnig, et al., Differential degradation of PIN2 auxin efflux carrier by retromer-dependent vacuolar targeting, Proc. Natl. Acad. Sci. U. S. A. 105 (2008) 17812–7. doi:10.1073/pnas.0808073105.

[22] T. Ischebeck, I. Stenzel, F. Hempel, X. Jin, A. Mosblech, I. Heilmann, Phosphatidylinositol-4,5-bisphosphate influences Nt-Rac5-mediated cell expansion in pollen tubes of Nicotiana tabacum, Plant J. 65 (2011) 453–468. doi:10.1111/j.1365-313X.2010.04435.x.

[23] E. Sundberg, L. Østergaard, Distinct and Dynamic Auxin Activities During Reproductive Development, Cold Spring Harb. Perspect. Biol. (2009) 1:a001628. doi:10.1101/cshperspect.a001628.

[24] M. Cardarelli, V. Cecchetti, Auxin polar transport in stamen formation and development: how many actors?, Front. Plant Sci. 5 (2014) 333. doi:10.3389/fpls.2014.00333.

[25] Z. Ding, B. Wang, I. Moreno, N. Dupláková, S. Simon, N. Carraro, et al., ER-localized auxin transporter PIN8 regulates auxin homeostasis and male gametophyte development in Arabidopsis, Nat. Commun. 3 (2012) 941. doi:10.1038/ncomms1941.

[26] N. Xu, X.-Q. Gao, X.Y. Zhao, D.Z. Zhu, L.Z. Zhou, X.S. Zhang, Arabidopsis AtVPS15 is essential for pollen development and germination through modulating phosphatidylinositol 3-phosphate formation, Plant Mol. Biol. 77 (2011) 251–60. doi:10.1007/s11103-011-9806-9.

[27] W.-Y. Wang, L. Zhang, S. Xing, Z. Ma, J. Liu, H. Gu, et al., Arabidopsis AtVPS15 plays essential roles in pollen germination possibly by interacting with AtVPS34, J. Genet. Genomics. 39 (2012) 81–92. doi:10.1016/j.jgg.2012.01.002.

[28] S. Serrazina, F.V. Dias, R. Malhó, Characterization of FAB1 phosphatidylinositol kinases in Arabidopsis pollen tube growth and fertilization, New Phytol. 203 (2014) 784–93. doi:10.1111/nph.12836.

[29] T. Hirano, T. Matsuzawa, K. Takegawa, M.H. Sato, Loss-of-function and gain-of-function mutations in FAB1A/B impair endomembrane homeostasis, conferring pleiotropic developmental abnormalities in Arabidopsis, Plant Physiol. 155 (2011) 797–807. doi:10.1104/pp.110.167981.

[30] T. Hirano, M.H. Sato, Arabidopsis FAB1A/B is possibly involved in the recycling of auxin transporters, Plant Signal. Behav. 6 (2011) 583–585. doi:10.4161/psb.6.4.15023.

[31] a Mayer, D. Scheglmann, S. Dove, A. Glatz, W. Wickner, A. Haas, Phosphatidylinositol 4,5-bisphosphate regulates two steps of homotypic vacuole fusion, Mol. Biol. Cell. 11 (2000) 807–817. doi:10.1091/mbc.11.3.807.

[32] R.A. Fratti, Y. Jun, A.J. Merz, N. Margolis, W. Wickner, B. Wickner, Interdependent assembly of specific regulatory lipids and membrane fusion proteins into the vertex ring domain of docked vacuoles, J. Cell Biol. 167 (2004) 1087–1098. doi:10.1083/jcb.200409068.

[33] F. Wiradjaja, L.M. Ooms, S. Tahirovic, E. Kuhne, R.J. Devenish, A.L. Munn, et al., Inactivation of the phosphoinositide phosphatases Sac1p and Inp54p leads to accumulation of phosphatidylinositol 4,5-bisphosphate on vacuole membranes and vacuolar fusion defects, J. Biol. Chem. 282 (2007) 16295–16307. doi:10.1074/jbc.M701038200.

[34] S. Elge, C. Brearley, H.-J. Xia, J. Kehr, H.-W. Xue, B. Mueller-Roeber, An Arabidopsis inositol phospholipid kinase strongly expressed in procambial cells: Synthesis of PtdIns(4,5)P2 and PtdIns(3,4,5)P3 in insect cells by 5-phosphorylation of precursors, Plant J. 26 (2001) 561–571. doi:10.1046/j.1365-313x.2001.01051.x.

[35] C. Zhang, G.R. Hicks, N. V Raikhel, Plant vacuole morphology and vacuolar trafficking, Front. Plant Sci. 5 (2014) 476. doi:10.3389/fpls.2014.00476.

[36] J. Wang, Y. Cai, Y. Miao, S.K. Lam, L. Jiang, Wortmannin induces homotypic fusion of plant prevacuolar compartments, J. Exp. Bot. 60 (2009) 3075–83. doi:10.1093/jxb/erp136.

[37] J. Zheng, S.W. Han, M.F. Rodriguez-Welsh, M. Rojas-Pierce, Homotypic vacuole fusion requires VTI11 and is regulated by phosphoinositides, Mol. Plant. 7 (2014) 1026–40. doi:10.1093/mp/ssu019.

[38] P. Baster, S. Robert, J. Kleine-Vehn, S. Vanneste, U. Kania, W. Grunewald, et al., SCF(TIR1/AFB)-auxin signalling regulates PIN vacuolar trafficking and auxin fluxes during root gravitropism, EMBO J. 32 (2013) 260–74. doi:10.1038/emboj.2012.310.

[39] M. Sauer, T. Paciorek, E. Benková, J. Friml, Immunocytochemical techniques for whole-mount in situ protein localization in plants., Nat. Protoc. 1 (2006) 98–103. doi:10.1038/nprot.2006.15.

FIGURE LEGENDS

Figure 1. *PIP5K1* and *PIPK2* are expressed in early stages of pollen development

Flowers of the indicated reporter lines and wild type were dissected under a binocular stereomicroscope. Pollen grains were extracted by squeezing the anthers over a glass slide and immediately imaged by confocal microscopy. Bright field (upper panel) and GFP fluorescence images (lower panel)are shown for each stage of pollen development. BCP: bicellular pollen; TCP: tricellular pollen. Arrowheads indicate GFP-positive nuclei fluorescence. Wild type Col-0 was used as a control for pollen autofluorescence. Scale bar is 10 µm

A. PIP5K1pro:nlsGUS-GFP

B. PIP5K2pro:nlsGUS-GFP

C. Wild type Col-0

Figure 2. Seed set depends on the function of *PIP5K1* and *PIP5K2* genes.

Mature siliques from different genotypes*PIP5K1* and *PIP5K2*mutant allele combinations lines were cleared in a solution of ethanol and acetic acid (9:1) and photographed under a binocular stereomicroscope. Arrowheads indicate empty sites indicative of failed fertilization events and the asterisk highlights a shrunken seed due to an embryo abortion.

Figure 3. Pollen abortion defect is tightly linked to the *PIP5K1* and *PIP5K2* functional genes

Pollen grains from open flowers of the indicated genotypes lines were observed by differential interphase contrast (DIC) microscopy. Normal and defective pollen grains were scored using the Alexander's staining method.

A, **B**. DIC-visualized pollen grains of wild type (A) and *pip5k1*$^{+/-}$*pip5k2*$^{+/-}$ (B) flowers. Scale bar is 10 µm.

C, **D**. Alexander stained pollen grains from wild type (C) and *pip5k1*$^{+/-}$*pip5k2*$^{+/-}$ (D) flowers. The arrowhead indicates a non-viable pollen grain which was not stained due to the absence of cytoplasm. Scale bar is 10 µm.

E. Quantification of pollen abortion of different combinations of *PIP5K1* and *PIP5K2* mutant alleles using Alexander staining. Results are shown as a percentage of the scored pollen grain in each line. n > 200.

Figure 4. Pollen abortion occurs early during microgametogenesis in *pip5k1*$^{+/-}$*pip5k2*$^{+/}$ mutants

Histological analysis of wild type and *pip5k1*$^{+/-}$ *pip5k2*$^{+/-}$ toluidine blue-stained transverse anther sections. Stages of anther development depicted as described by Sanders et al., 1999 [14].

A. Wild type stage 5 anthers.

B. Wild type dehiscent anthers, stage 13.

C. *pip5k1*$^{+/-}$ *pip5k2*$^{+/-}$ stage 5 anther

D. *pip5k1*$^{+/-}$ *pip5k2*$^{+/-}$ dehiscent (stage 13) anthers with mature pollen grains

Black arrowheads in C and D indicate aborted pollen grains which appear as early as the tetrad stage in double mutants. ep: epidermis, en: endothecium, ml: middle layer, t: tapetum, MMC: microspore mother cells, PG: pollen grain.

Figure 5. Vacuole biogenesis is defective in mature pollen grains of the *pip5k1*$^{+/-}$ *pip5k2*$^{+/-}$ mutant.

A-**B**. Neutral Red staining of mature pollen grains from wild type (A) and *pip5k1*$^{+/-}$ *pip5k2*$^{+/-}$ (B) plants. Arrowheads indicate abnormally large vacuoles in pollen grains. Bar size = 10 µm.

C-**H**. Transmission electron microscopy (TEM) analysis of pollen grains obtained from wild type (C, E, F) and *pip5k1*$^{+/-}$ *pip5k2*$^{+/-}$(D, G, H) plants. Defects in vacuole morphology are indicated with black arrowheads in F and H. Also defect in exine formation is observed (arrowheads in E and G). N: nuclei; Nuc: nucleolus; V: vacuole; m: mitochondria. Scale bar is 3 µm in E- H and 5 µm in C-D.

Figure 6. Root tip cells of *pip5k1*$^{-/-}$*pip5k2*$^{-/-}$displays defects in vacuole morphology and endocytic trafficking.

A. Lysotracker Red staining of 7 day-old wild type and *pip5k1*$^{-/-}$*pip5k2*$^{-/-}$ seedling root tips. Bar size = 20 µm.

B. Whole mount root immunolocalization using antiPIN1 antibody in wild type and *pip5k1*$^{-/-}$ *pip5k2*$^{-/-}$ treated with 25 (BFA25) or 50 µM (BFA50) Brefeldin A for 90 minutes. Bar size = 20 µm.

C. PIN1 positive BFA body area quantification.* Two-tailed Student's *t*-Test $P < 0.01$.

SUPPLEMENTARY INFORMATION

Supplementary Figure S1. *PIP5K1* and *PIP5K2* expression levels in different tissues of *Arabidopsis* plants and auxin treated pollen grains

A. *PIP5K1* and *PIP5K2* mRNA in different tissues was determined by RT-qPCR.

B. Pollen grains were treated with IAA or control condition in the presence or absence of CHX. Transcript levels of *PIP5K1* and *PIP5K2* were determined by RT-qPCR. The results are expressed relative to the housekeeping gene.

Supplementary Table 1.*PIP5K* transcript levels during microgametogenesis. Normalized absolute *PIP5K* transcript values obtained from the data published by Honys and Twell, 2004 [8] in different stages of microgametogenesis**.** Unicellular microspore (UNM), bicellular pollen (BCP), tricellular pollen (TCP) and mature pollen grains (MPG).

Supplementary Table 2. Expected and experimental segregation of male gamete abortion. Two genetic scenarios are shown. (A) Fully penetrance for each mutant allele, and (B) Combination of the any pair of mutant alleles resulting in pollen lethality. Values are expressed as percentage.

Supplementary Table 3. List of primers used for *PIP5K*stranscript levelanalyses and genotyping of the *PIP5K*T-DNA insertional mutants.

Figure(s)

1

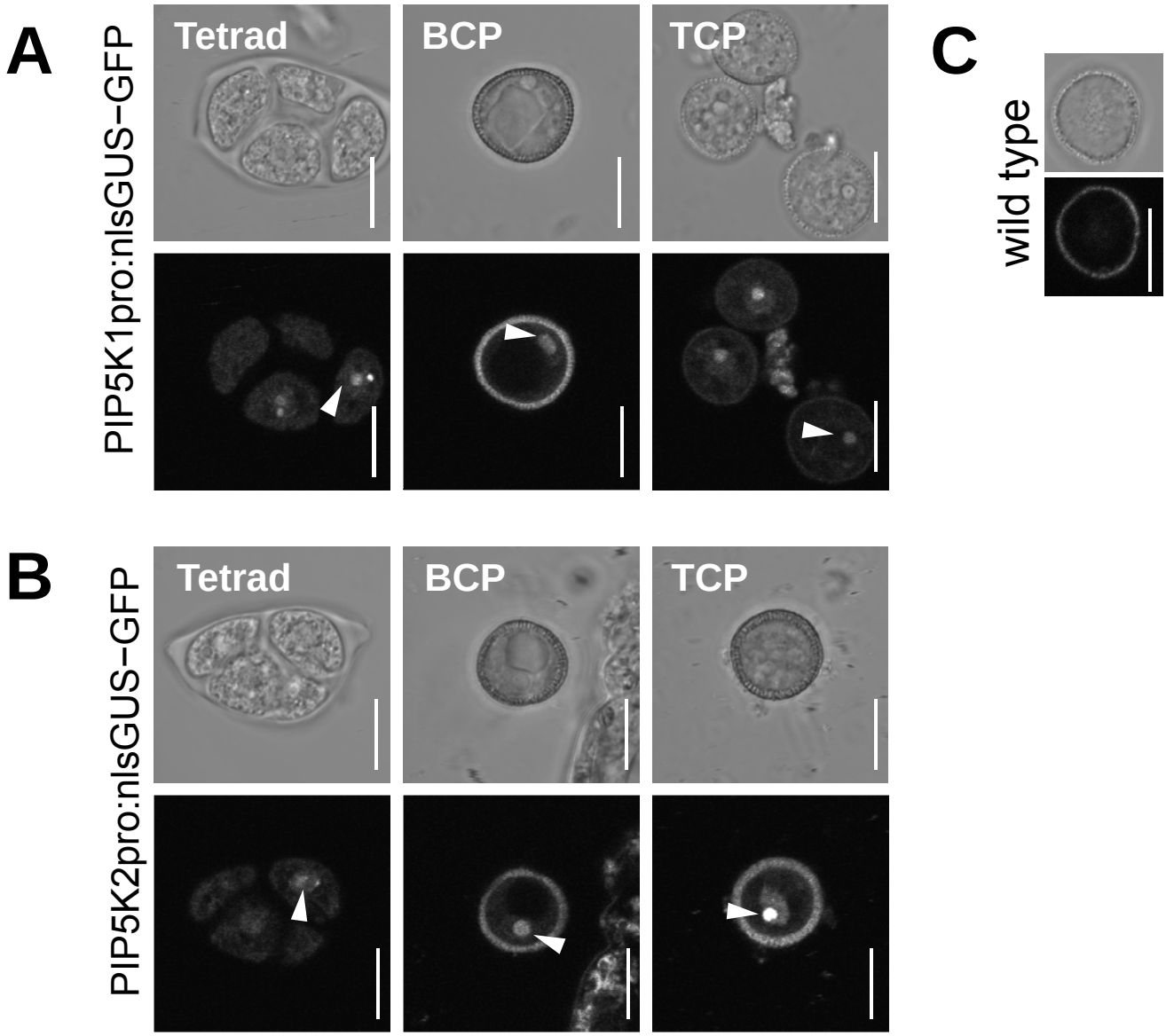

Figure 1. *PIP5K1* and *PIPK2* are expressed in early stages of pollen development

Flowers of the indicated reporter lines and wild type were dissected under a binocular stereomicroscope. Pollen grains were extracted by squeezing the anthers over a glass slide and immediately imaged by confocal microscopy. Bright field (upper panel) and GFP fluorescence images (lower panel)are shown for each stage of pollen development. BCP: bicellular pollen; TCP: tricellular pollen. Arrowheads indicate GFP-positive nuclei fluorescence. Wild type Col-0 was used as a control for pollen autofluorescence. Scale bar is 10 µm

A. PIP5K1pro:nlsGUS-GFP

B. PIP5K2pro:nlsGUS-GFP

C. Wild type Col-0’

2

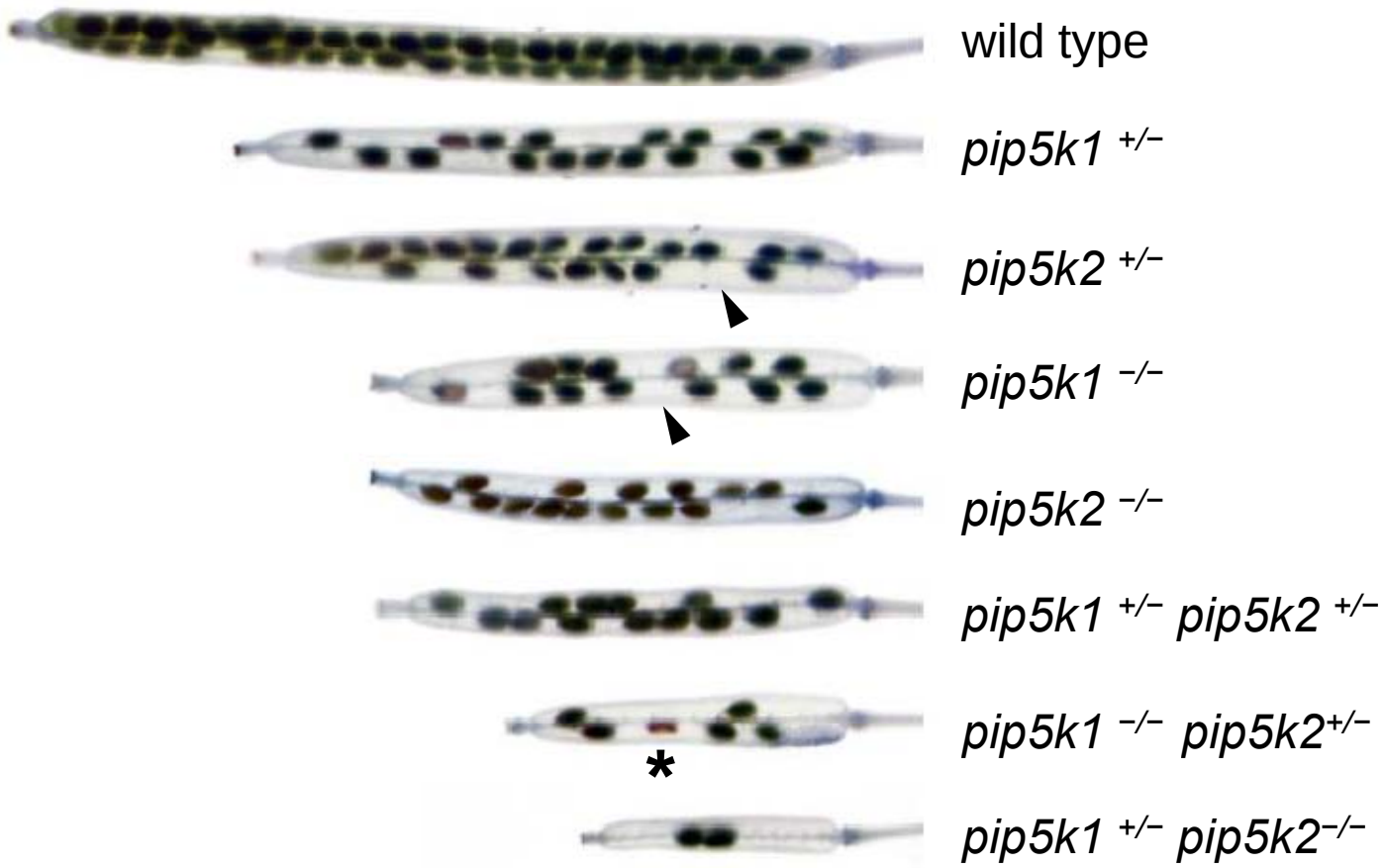

Figure 2. Seed set depends on the function of *PIP5K1* and *PIP5K2* genes.
Mature siliques from different genotypes*PIP5K1* and *PIP5K2*mutant allele combinations lines were cleared in a solution of ethanol and acetic acid (9:1) and photographed under a binocular stereomicroscope. Arrowheads indicate empty sites indicative of failed fertilization events and the asterisk highlights a shrunken seed due to an embryo abortion.

3

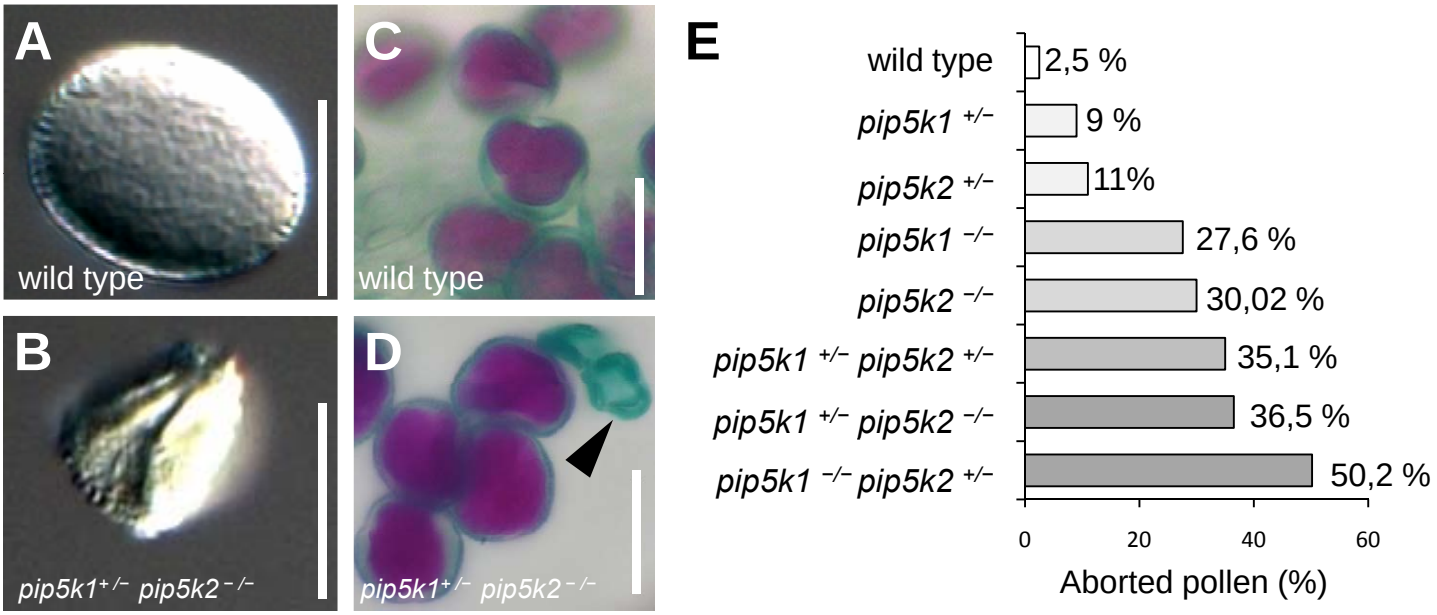

Figure 3. Pollen abortion defect is tightly linked to the *PIP5K1* and *PIP5K2* functional genes
Pollen grains from open flowers of the indicated genotypes lines were observed by differential interphase contrast (DIC) microscopy. Normal and defective pollen grains were scored using the Alexander's staining method.
A, **B**. DIC-visualized pollen grains of wild type (A) and *pip5k1*$^{+/-}$*pip5k2*$^{+/-}$ (B) flowers. Scale bar is 10 µm.
C, **D**. Alexander stained pollen grains from wild type (C) and *pip5k1*$^{+/-}$*pip5k2*$^{+/-}$ (D) flowers. The arrowhead indicates a non-viable pollen grain which was not stained due to the absence of cytoplasm. Scale bar is 10 µm.
E. Quantification of pollen abortion of different combinations of *PIP5K1* and *PIP5K2* mutant alleles using Alexander staining. Results are shown as a percentage of the scored pollen grain in each line. n > 200.

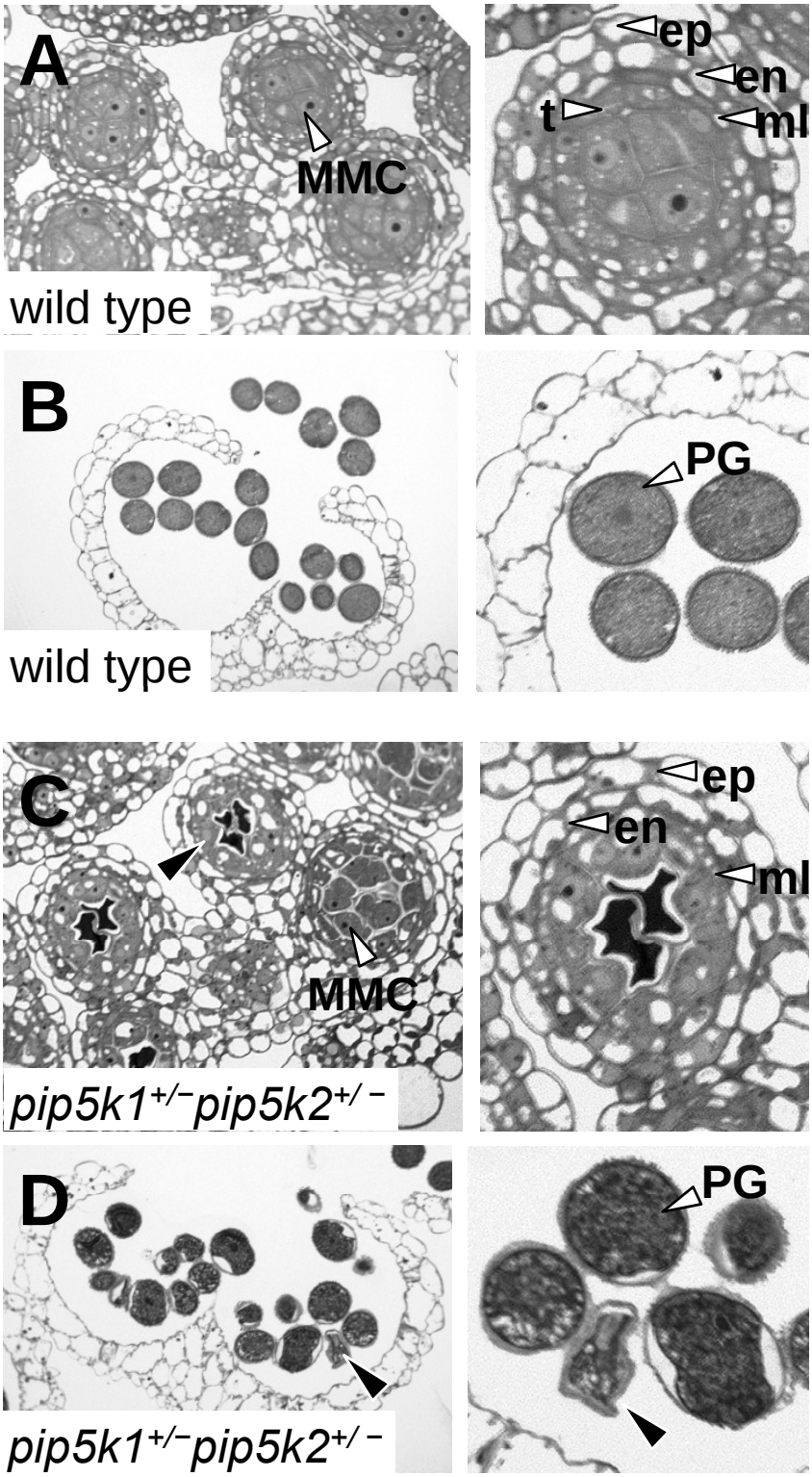

Figure 4. Pollen abortion occurs early during microgametogenesis in *pip5k1*$^{+/-}$*pip5k2*$^{+/}$ mutants
Histological analysis of wild type and *pip5k1*$^{+/-}$ *pip5k2*$^{+/-}$ toluidine blue-stained transverse anther sections. Stages of anther development depicted as described by Sanders et al., 1999 [14].
A. Wild type stage 5 anthers.
B. Wild type dehiscent anthers, stage 13.
C. *pip5k1*$^{+/-}$ *pip5k2*$^{+/-}$ stage 5 anther
D. *pip5k1*$^{+/-}$ *pip5k2*$^{+/-}$ dehiscent (stage 13) anthers with mature pollen grains
Black arrowheads in C and D indicate aborted pollen grains which appear as early as the tetrad stage in double mutants. ep: epidermis, en: endothecium, ml: middle layer, t: tapetum, MMC: microspore mother cells, PG: pollen grain.

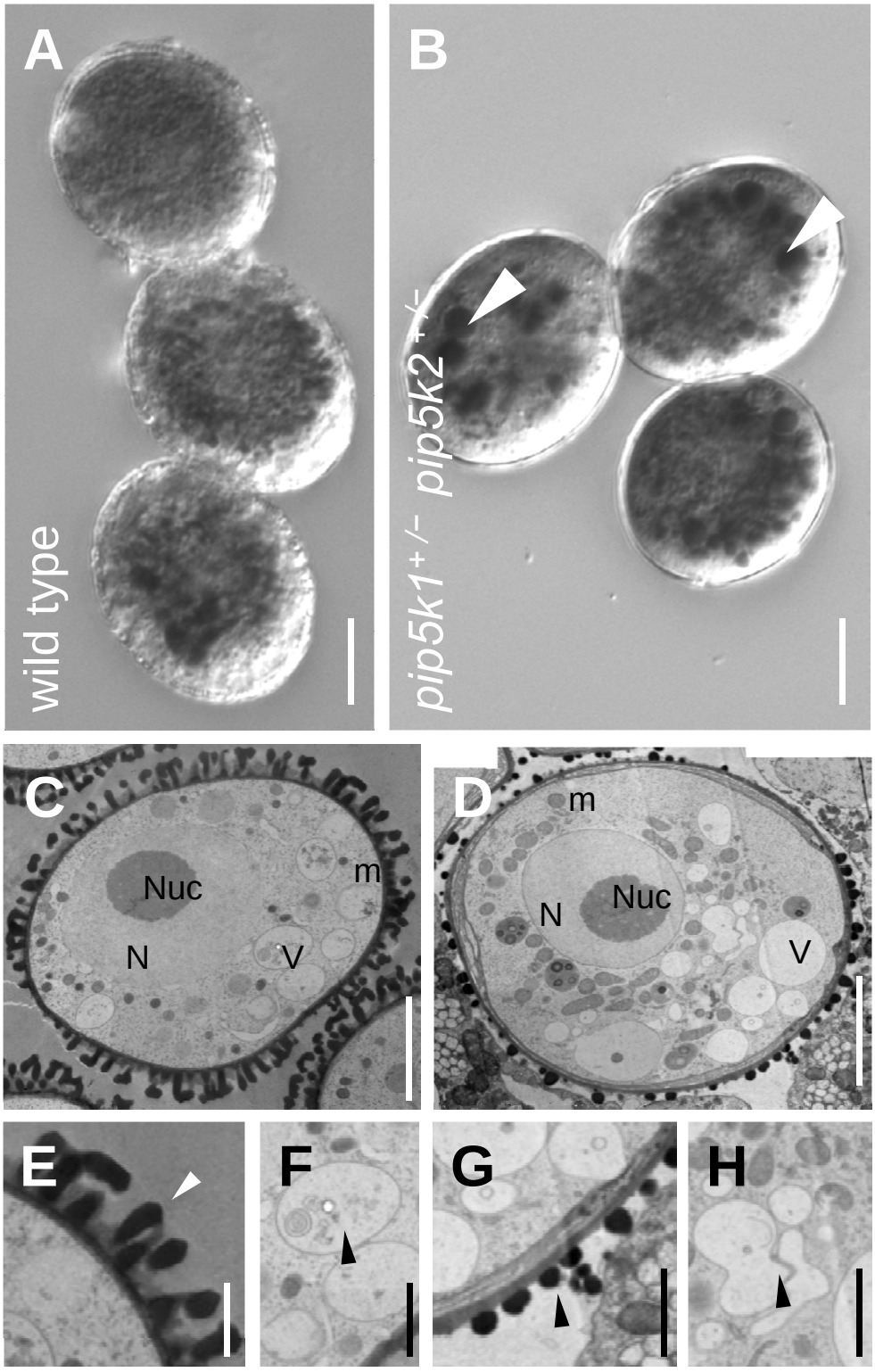

Figure 5. Vacuole biogenesis is defective in mature pollen grains of the *pip5k1*$^{+/-}$ *pip5k2* $^{+/-}$ mutant.
A-**B**. Neutral Red staining of mature pollen grains from wild type (A) and *pip5k1*$^{+/-}$ *pip5k2* $^{+/-}$ (B) plants. Arrowheads indicate abnormally large vacuoles in pollen grains. Bar size = 10 µm.
C-**H**. Transmission electron microscopy (TEM) analysis of pollen grains obtained from wild type (C, E, F) and *pip5k1*$^{+/-}$ *pip5k2*$^{+/-}$(D, G, H) plants. Defects in vacuole morphology are indicated with black arrowheads in F and H. Also defect in exine formation is observed (arrowheads in E and G). N: nuclei; Nuc: nucleolus; V: vacuole; m: mitochondria. Scale bar is 3 µm in E- H and 5 µm in C-D.

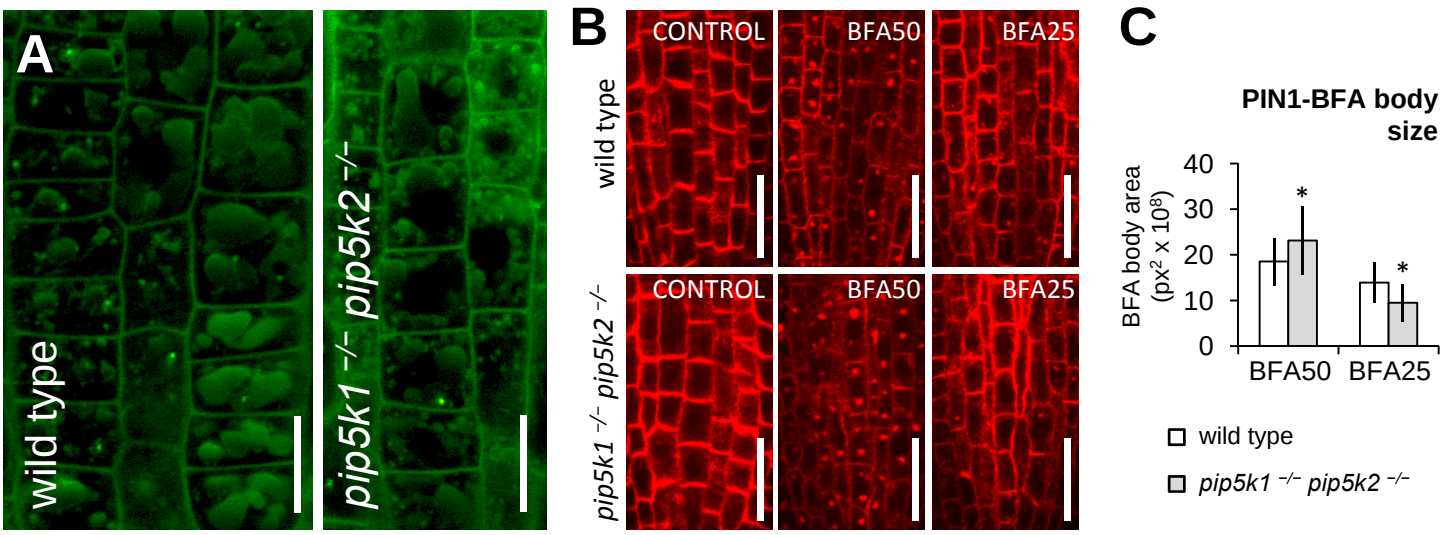

Figure 6. Root tip cells of *pip5k1*$^{-/-}$*pip5k2*$^{-/-}$ displays defects in vacuole morphology and endocytic trafficking.

A. Lysotracker Red staining of 7 day-old wild type and *pip5k1*$^{-/-}$*pip5k2*$^{-/-}$ seedling root tips. Bar size = 20 µm.

B. Whole mount root immunolocalization using antiPIN1 antibody in wild type and *pip5k1*$^{-/-}$ *pip5k2*$^{-/-}$ treated with 25 (BFA25) or 50 µM (BFA50) Brefeldin A for 90 minutes. Bar size = 20 µm.

C. PIN1 positive BFA body area quantification.* Two-tailed Student's *t*-Test $P < 0.01$.

SUPPLEMENTARY INFORMATION

Supplementary figure S1. *PIP5K1/2* expression profiles in different tissues of *Arabidopsis* plants and auxin inducibility in pollen grains

A. qRT-PCR of *PIP5K1* and *PIP5K2* mRNA in different tissues. RNA samples from roots, steams, leaves and closed or open flowers.

B. Transcript levels of *PIP5K1* and *PIP5K2*in pollen grains were determined by qRT-PCR after treatment with IAA or the mock control in the presence or absence of CHX.

Table Supplementary 1. PIP5K expression levels during microgametogenesis. Unicellular microspore (UNM), Bicellular pollen (BCP), tricellular pollen (TCP) and Mature pollen grain (MPG). The data represents normalized absolute values as described in Honys and Twell, 2004.

Table Supplementary 2. Comparison of observed and expected segregation of male gamete abortion in two scenarios: one in which each mutant allele is fully penetrant by its own (A) and other where only the combination of the two mutant alleles generates pollen lethality (B). Values are expressed in percentage

Table Supplementary 3. List of primes used for expression analyses and genotyping the pip5k T- DNA insertional mutants.

S1

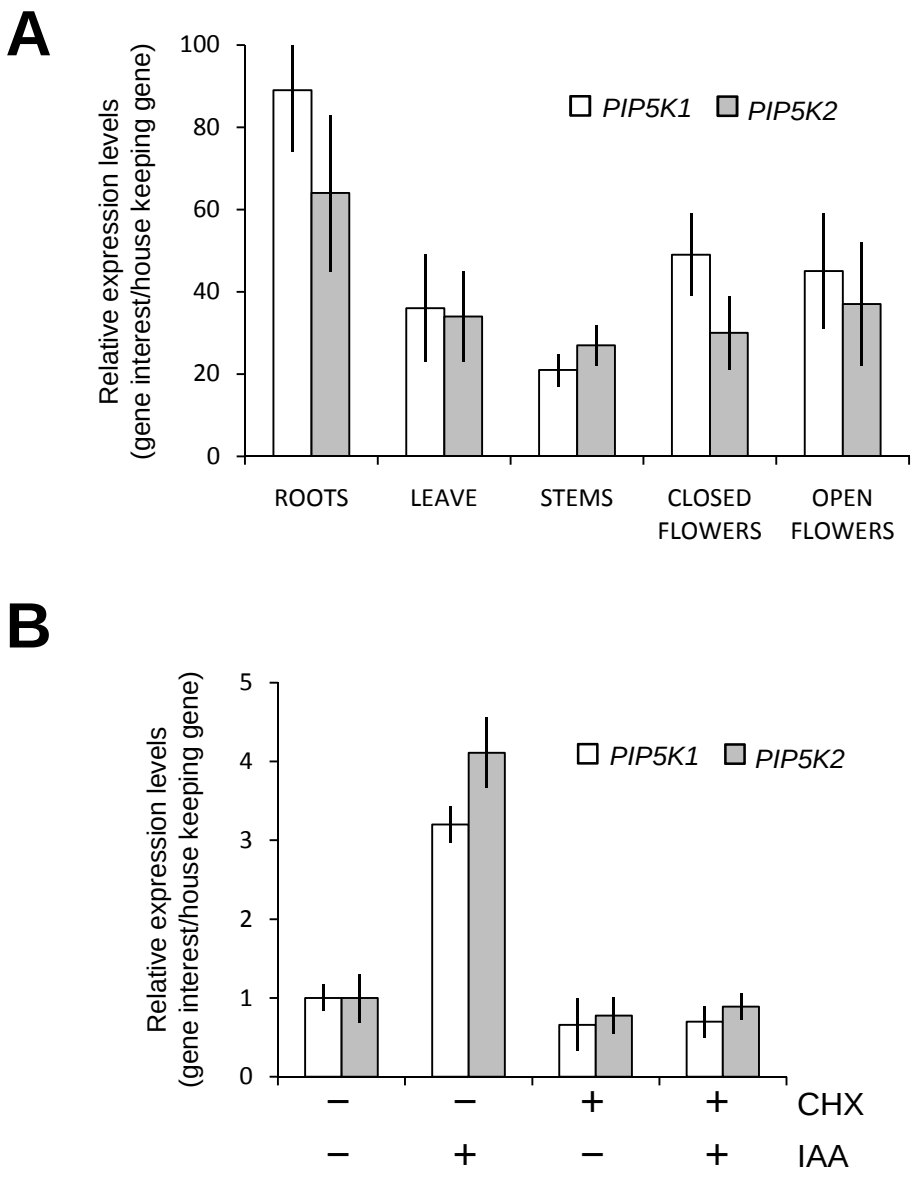

Supplementary figure 1. *PIP5K1/2* expression profiles

A. qRT-PCR detection of PIP5K1 and PIP5K2 mRNA in different tissues. RNA samples from roots, steams, leaves and closed or open flowers.

B. mRNA levels of PIP5K1 and PIP5K2 were determined by qRT-PCR after treatment with IAA or CHX.

Supplementary table 1. *PIP5K* expression levels during microgametogenesis. Unicellular microspore (UNM), Bicellular pollen (BCP), tricellular pollen (TCP) and Mature pollen grain (MPG). The data represents normalized absolute values as described in Honys and Twell, 2004.

		Developmental Stage			
		UNM	**BCP**	**TCP**	**MPG**
PIP5K1	At1g21980	0	166	0	0
PIP5K2	At1g77740	127	132	0	0
PIP5K3	At2g26420	0	0	0	0
PIP5K4	At3g56960	66	180	1496	1281
PIP5K5	At2g41210	144	254	2048	1585
PIP5K6	At3g07960	309	349	1470	1609
PIP5K7	At1g10900	0	0	0	0
PIP5K8	At1g60890	441	417	470	538
PIP5K9	At3g09920	0	0	0	0
PIP5K10	At1g01460	0	0	1250	3103
PIP5K11	At4g01190	224	226	0	0

Supplementary table 2. Comparison of observed and expected segregation of male gamete abortion in two scenarios: one in which each mutant allele is fully penetrant by its own (A) and other where only the combination of the two mutant alleles generates pollen lethality (B). Values are expressed in percentage.

		Observed		Expected Aborted pollen grains	
pip5k1	***pip5k2***	**normal**	**aborted**	**A**	**B**
+/+	+/+	97.5	2.5	0	0
−/+	+/+	91	9	50	0
+/+	−/+	89	11	50	0
−/−	+/+	72.4	27.6	100	0
+/+	−/−	69.98	30.02	100	0
+/−	+/−	64.9	35.1	75	25
+/−	−/−	63.5	36.5	100	50
−/−	+/−	49.8	50.2	100	50

Supplementary table 3. List of primes used for expression analyses and genotyping the *pip5k* T-DNA insertional mutants.

Primer name	Sequence (5’ –> 3’)	Use
PIP5K1-GT-F	AAGATGGGTGCATGTACGAA	Mutant Genotyping
PIP5K1-GT-R	TTCCACCTGAAA TCCACTGA	Mutant Genotyping
PIP5K2-GT-F	GGAAGTTTGACTGGGGAGAAG	Mutant Genotyping
PIP5K2-GT-R	TCATACTGGCAGACGTGTTTG	Mutant Genotyping
LB1.3	ATTTTGCCGA TTTCGGAAC	Mutant Genotyping
PIP5K1-qPCR-F	GCGGGAAGAGTAAAAAGGTAAATC	Gene Expression
PIP5K1-qPCR-R	CCTCCCCAACCCAAAAACTT	Gene Expression
PIP5K2-qPCR-F	GCATTAGGGGCAAAAGGGT	Gene Expression
PIP5K2-qPCR-R	AAATAAGTAATCCCCCACCCAA	Gene Expression
PPR-F (HK)	AAGACAGTGAAGGTGCAACCTTACT	Gene Expression
PPR-R (HK)	AGTTTTTGAGTTGTATTTGTCAGAGAAAG	Gene Expression

REFERENCES

Honys, D. and Twell, D. (2004). Transcriptome analysis of haploid male gametophyte development in Arabidopsis. Genome Biol. **5**: R85.